Nanoplasticity of Single-Wall Carbon Nanotubes under Uniaxial Compression

Deepak Srivastava,[1,*] Madhu Menon,[2,3,†] and Kyeongjae Cho[4,‡]

[1]*NASA Ames Research Center, MS T27A-1, Moffett Field, California 94035-1000*
[2]*Department of Physics and Astronomy, University of Kentucky, Lexington, Kentucky 40506-0055*
[3]*Center for Computational Sciences, University of Kentucky, Lexington, Kentucky 40506-0045*
[4]*Department of Mechanical Engineering, Stanford University, California 94305-4040*

(Received 16 April 1999)

Nanoplasticity of thin single-wall carbon nanotubes under uniaxial compression is investigated using generalized tight-binding molecular dynamics, and *ab initio* electronic structure methods. A novel mechanism of nanoplasticity of carbon nanotubes under uniaxial compression is observed in which bonding geometry collapses from a graphitic (sp^2) to a localized diamondlike (sp^3) reconstruction. The computed critical stress ($\approx$153 GPa) and the shape of the resulting plastic deformation is in good agreement with recent experimental observations.

PACS numbers: 61.48.+c, 62.20.Fe

The discovery of carbon nanotubes (CNT) by Iijima [1,2] and subsequent observations of CNT's unique mechanical and electronic properties have initiated intensive research on these quasi-one-dimensional structures. CNTs have been identified as one of the most promising building blocks for future development of functional nanostructures. Accurate characterization of nanomechanics in the elastic and plastic regimes, therefore, is highly desirable for any application in nanocomposites and/or devices. As external stress is applied to nanotubes, initial linear elastic deformations are observed up to a certain critical strain beyond which nonlinear responses set in. In the nonlinear response regime, locally deformed structures such as pinches, kinks, and buckles have been observed in both experiments and simulations [3–12].

Classical molecular dynamics (MD) simulations, employing Tersoff-Brenner many-body atomistic interactions [13,14] performed for single and multiwalled CNT under tensile and compressive stresses show them to be extremely elastic, well beyond the typical yield strain of 0.1% for most other materials [7,9]. Surprisingly, compressed CNT in the nonlinear elastic response regime are also shown to completely recover from severe structural deformations such as localized pinches and kinks [7,9,12]. Under tensile strain, a plastic response behavior primarily driven by Stone-Wales (SW) bond rotation defects [15], which generate pentagon-heptagon (5/7) pair defects in a graphene lattice, has been proposed [16–18]. It is suggested that the axially compressed CNT would also behave similarly and deform plastically via SW defect formation mechanism [16]. The classical MD simulations of compressed nanotubes, performed so far, however, show only completely elastic deformation up to 15% and higher strain for similar tubes [7,9,12]. In these simulations, CNT behave as elastic rods that pinch and buckle locally into a variety of morphological patterns that were predicted in a continuum mechanics based shell model description of the nanomechanics [7].

In a recent experiment, large compressive strains were applied to CNT dispersed in composite polymeric films. Two distinct deformation modes, sideways buckling of thick tubes and collapse/fracture of thin tubes without any buckling, have been observed [19]. While the buckling of thick tubes is in qualitative agreement with the classical MD simulations [7], the plastic collapse or fracture of thin tubes without any buckling is contrary to these simulations [7,9,16]. The compressive strain in the experiment is estimated to be larger than 5%, and critical stress for inward collapse or fracture is expected to be 100–150 GPa for thin tubes [19].

In this Letter, we investigate the plasticity of compressed nanotubes using the quantum generalized tight-binding molecular dynamics (GTBMD) scheme of Menon and Subbaswamy [20]. The method has been found to be very reliable in obtaining good agreement with experimental results for the structural and vibrational properties of fullerenes and nanotubes [20,21]. We report collapse and plasticity of compressed thin nanotubes via graphitic (sp^2) to diamondlike (sp^3) bonding reconstruction at the location of the collapse that is driven by the relaxation of the accumulated strain energy in the uncollapsed section of the tube. The nature of the collapse is in qualitative agreement with the experimental observation of Lourie *et al.* and the estimated critical stress ($\approx$153 GPa) is also within the experimentally determined range [19].

The axial compression of an (8, 0) CNT is achieved by keeping the edge atoms of the tube transparent to the forces generated in the GTBMD method. The positions of the edge atoms are moved axially inward at a fixed rate to compress the nanotube. Each 1% compression in the linear response regime, and 0.25% compression near elastic limit, is accompanied by a GTBMD relaxation. Keeping the strained atoms fixed, the edge atoms are then adjusted and relaxed. At the elastic limit [for 12% compression of (8, 0) CNT], the relaxation of the compressed tube resulted in a spontaneous plastic collapse.

The compressed nanotube energetics during the collapse was analyzed with an *ab initio* density functional theory (DFT) using pseudopotential method [22]. The strain energy per atom is calculated as the difference in the total energy per atom of the strained and unstrained tube, as a function of percentage strain, and is shown in Fig. 1a. For comparison, in the same figure, we also show the similar strain energy calculated from classical MD simulations [14]. Parabolic fits to two sets of data in the linear elastic response regime is used to compute the Young's modulus for the nanotube. The calculated value from the GTBMD method is 1.3 TPa (using 3.4 Å for the CNT thickness) for the $(8, 0)$ nanotube considered. For low value of compressive strain ($\leq 8\%$), before any structural deformation occurs, the classical MD values are also in reasonably good agreement with the quantum GTBMD values as shown in Fig. 1a. Significant differences, however, begin to occur for compressive strain larger than 8%. While the GTBMD curve (Fig. 1a) shows that the $(8, 0)$ nanotube can be compressed up to 12 (± 0.25)% before any structural deformation occurs, the classical MD simulation for the same nanotube shows the structural deformation to start between 8% and 9%. Moreover, the nature of the structural deformation in the two cases is also significantly different. The structural deformation at 12% strain (as shown in Fig. 1b) in the quantum GTBMD method is completely spontaneous and leads to plastic collapse of the tube. The structural deformation in the classical MD method (observed between 8%–9% strain) resulting in the formation of symmetric-pinching modes, on the other hand, is completely elastic [23].

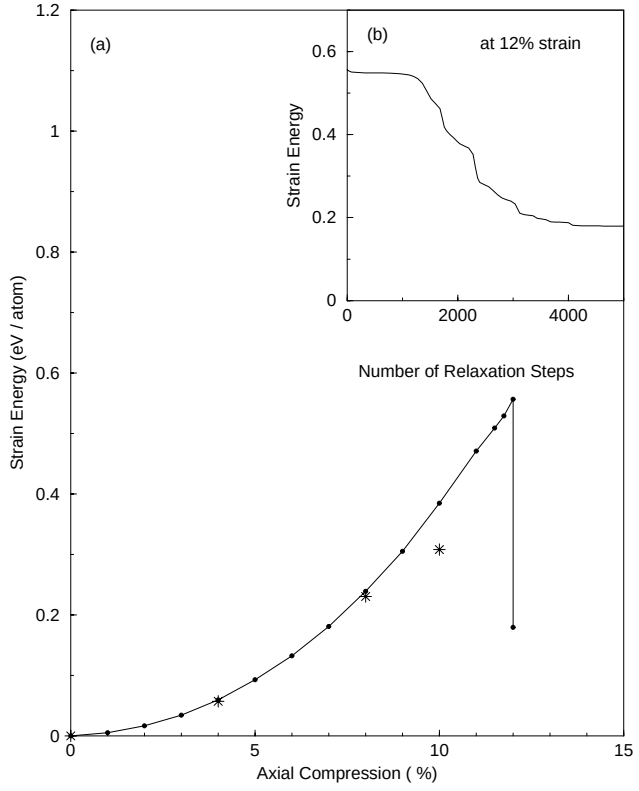

FIG. 1. (a) Strain energy as a function of strain in an axially compressed $(8, 0)$ nanotube. Filled circles are for compression computed with the quantum GTBMD method, whereas stars are for the values computed with classical MD method. Inset (b) shows the strain energy minimization at 12% strain as a function of number of GTBMD relaxation steps.

Microscopic details and mechanism of the structural collapse are discussed next. At 12% strain, as shown in Fig. 2a, structural deformation starts asymmetrically at two locations in the tube with small changes in an otherwise circular cross section. Strain relaxation in the center (highly strained) region of the tube forces the atoms, at the locations of the deformations, to gradually collapse inward as shown in Figs. 2b and 2c. Fourfold coordinated bonds are formed and the structure is further "pulled" inwards by the newly formed (sp^3-type) bonds (Fig. 2d). The energetics of the spontaneous inward collapse (shown in Fig. 1b), as discussed above, show that there is a net energy release for this process.

The structural changes during the CNT collapse are further illustrated in a radial distribution function (RDF) analysis that is shown in Figs. 3a and 3b. For simplicity, only the RDF peak around first neighbor shell radial distance is discussed. At 0% compression there is a single peak near the equilibrium carbon-carbon (sp^2-type) bond distance of 1.42 Å in an unstrained graphene sheet. At 4% compression a second peak, representing compressed bonds along the tube axis, develops at about 1.37 Å. The

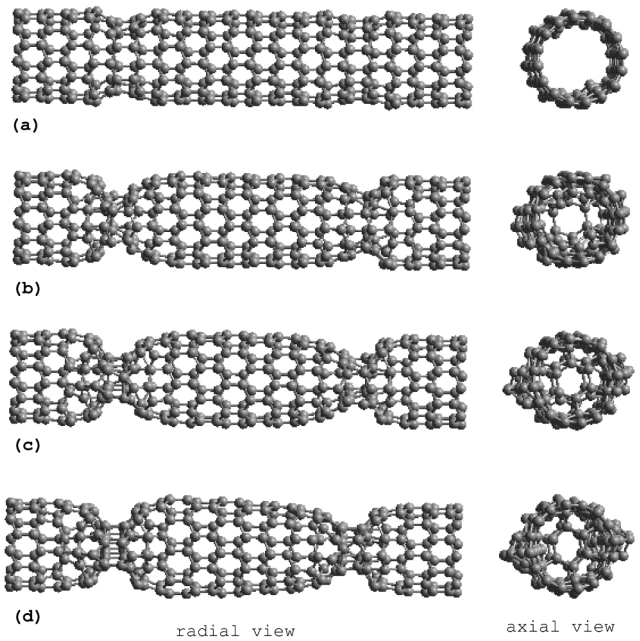

FIG. 2. Four stages of spontaneous plastic collapse of the 12% compressed $(8, 0)$ carbon nanotube showing: (a) nucleation of the deformations; [(b) and (c)] inward collapse at the locations of deformations; and (d) graphitic to diamondlike structural transition at the location of the collapse.

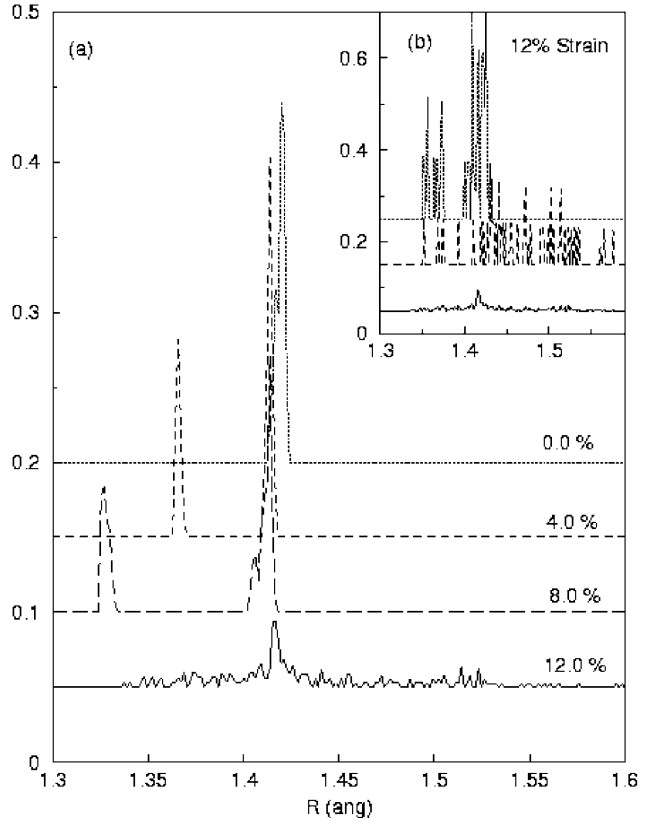

FIG. 3. Radial distribution function (RDF) near first neighbor shell as a function of radial distance. (a) RDF at 0%, 4%, 8%, and 12% compressed and GTBMD energy minimized tube, and (b) contributions to 12% compressed tube RDF from central uncollapsed and two collapsed sections of the tube.

original peak with a reduced magnitude also shifts to a lower value of 1.41 Å. This indicates that most of the axial strain is borne by the bonds parallel to the tube axis. The remaining strain has been used up in altering the bond angles and in increasing the tube radius as defined by the Poisson ratio. At 8% strain the second peak, representing strained bonds parallel to the tube axis, shifts to about 1.33 Å, while the first peak, representing unstrained bonds, remains practically unaffected. At 12% strain onset of the structural collapse is seen (Fig. 2d) accompanied by the vanishing of the second peak representing strained bonds parallel to the tube axis. The original peak, representing mostly the uncollapsed section, is also significantly reduced in magnitude. Many smaller peaks (like a background noise-type distribution of bond lengths) in the range 1.34–1.60 Å are observed. This signifies a breakdown of the starting (strained or unstrained) sp^2-type bonding structure.

The dotted line in the background in Fig. 3b shows that the uncollapsed section still preserves the two peak structure, the original peak representing nonaxially aligned nonstrained bonds at around 1.42 Å and the strained (but split) peak around 1.36 Å representing axially aligned strained bonds in the uncollapsed section. This indicates a reduction in the strain in the uncollapsed section from 12% to 4%. The dashed line in the middle representing the collapsed section shows a wide distribution (1.42–1.55 Å) of bond lengths. The lower edge near 1.42 Å represents sp^2-type bonds of the original but collapsed graphene tube while the upper edge near 1.55 Å represents compressed sp^3-type bonds of diamondlike reconstruction shown in Fig. 2d.

The collapsed part (left section in Fig. 2d) contains 6 fourfold coordinated atoms that induce a significant reduction (from 7.4 to 6.1 Å) in the axial length of this section. The *ab initio* energetics of the collapsing section shown in Figs. 2a–2d reveals that there is net 3.0 eV energy increase in the collapsed section, and a local activation barrier of about 8.4 eV to the collapse. Comparing the energetics of the same section with the value at the beginning of the collapse leads to an effective spring constant of $K = 5171.6$ eV/Å^2 ($\Delta E = K\epsilon^2/2$). This corresponds to a Young's modulus of 1.4 TPa before collapse and a net length reduction of about 1.3 Å due to the collapse. The accumulated axial strain in the uncollapsed section, on the other hand, is simultaneously reduced, providing the driving force for the observed mechanism as well. The estimated strain energy release in the uncollapsed section ($\approx$50 eV estimated from the effective spring constant) for the uncollapsed section is large enough to overcome the estimated local activation barrier and deposit an extra strain energy of magnitude 3 eV in the compressed collapsed section. The remaining released strain energy of the uncollapsed section is dissipated in the form of heat and is removed by the GTBMD energy minimization process. Thus, there is a net strain energy release through the local collapsing process.

Even though our analysis is based on simulations for short length CNT (320 atoms containing $N = 5$ units of 64 atoms each), we can generalize it to longer length CNT. Assuming that the CNT could experience a similar collapse, and that each unit in the collapsed part is compressed by the same (1.3 Å) amount with an equivalent release of strain in the uncollapsed part, we can estimate the strain energy released for a longer uncollapsed part. The strain on the uncollapsed part is 12% before the collapse and is reduced by $(1.3/N)/8.7$ due to collapse, where there are N units (of 64 atoms each) of uncollapsed nanotube with each unit measuring 8.7 Å before the collapse. The residual strain on the uncollapsed part is $\epsilon = 0.12 - (1.3/8.7)/N$ and the net strain energy change is $-37.2 \times (2.5N - 1.6)/N$ eV, where we have used the value of the spring constant estimated earlier. The longer $(8, 0)$ CNT in the large-N limit, thus, will release 93 eV per collapsed unit of the nature described above. The net strain energy release (93 eV per collapse) is thus still large enough to overcome any local activation energy barriers for collapse or even lead to fracture without any buckling [19].

In the above analysis we have assumed that the mechanism of the collapse remains unchanged as the tube length

increases. A simple estimation of the Euler buckling stress for the length (≈4 nm) of the tube used in this simulation shows that the critical stress needed for buckling or other morphological deformations is about twice as much as the value at which the tube has collapsed in our work. For longer tubes, however, the needed critical stress for Euler buckling will be less, and could compete with the above collapsing or plastic deformation mechanism. Similarly, a larger diameter tube of similar length could also be compressed to first undergo Euler buckling before neighboring carbon atoms start to interact, strongly causing the inward collapse of the structure from sp^2- to sp^3-type reconstruction. This explains the observation of both buckling of thick tubes and collapse/fracture without buckling of thin tubes in the experiment [19].

In summary, we have presented a novel nanoplastic mechanism of compressed nanotubes where local tetrahedral bonds (sp^3) of carbon atoms form at the location of the collapse. This is also reminiscent of graphitic to diamondlike phase transition observed in high compressive pressure cells (≈150 GPa) in the core of irradiated and annealed bucky onions [24]. The computed critical stress (≈153 GPa for 12% compressed tube) is in good agreement with the experimentally estimated range of values reported by Lourie *et al.* for thin nanotubes [19]. Most significantly, our work considerably lowers the elastic limit for thin compressed nanotubes (to within 12%) as compared to the 15% and higher values computed by the classical MD atomistic simulations [7,9]. The classical MD simulations employing Tersoff-Brenner potential for the same nanotube never plastically deform the nanotube, even at larger compression, by the mechanism described in this work. This is because morphological deformations such as symmetric pinches and sideways buckles form first and additional strain is accommodated by the extended sideways buckles.

Part of this work (D. S.) is supported by MRJ under NASA Contract No. NAS2-14303. M. M. acknowledges support through grants by NSF (OSR 99-07463), DEPSCoR (OSR 99-63231 and OSR 99-63232), and the Semiconductor Research Corporation (SRC). K. C.'s work is supported by Stanford's Terman Award from the Packard Foundation and the NSF-MRSEC. The *ab initio* computations are performed on T90 allocated through the NPACI Grant "Nanoscale Materials Simulations."

*Email address: deepak@nas.nasa.gov
†Email address: super250@pop.uky.edu
‡Email address: kjcho@stanford.edu

[1] S. Iijima, Nature (London) **354**, 56 (1991).
[2] S. Iijima and T. Ichihashi, Nature (London) **363**, 603 (1993); D. S. Bethune, C.-H. Kiang, M. S. deVries, G. Gorman, R. Savoy, J. Vazquez, and R. Beyers, Nature (London) **363**, 605 (1993).
[3] S. Iijima, C. Brabec, A. Maiti, and J. Bernholc, J. Chem. Phys. **104**, 2089 (1996).
[4] J. Despres, E. Daguerre, and K. Lafdi, Carbon **33**, 87 (1995).
[5] N. Chopra, L. Benedict, V. Crespi, M. L. Cohen, S. G. Louie, and A. Zettl, Nature (London) **377**, 135 (1995).
[6] R. Ruoff and D. Lorents, Bull. Am. Phys. Soc. **40**, 173 (1995).
[7] B. I. Yakobson, C. J. Brabec, and J. Bernholc, Phys. Rev. Lett. **76**, 2511 (1996).
[8] M. R. Falvo, G. J. Clary, R. M. Taylor II, V. Chi, F. P. Brooks, Jr., S. Washburn, and R. Superfine, Nature (London) **389**, 582 (1997).
[9] D. Srivastava and S. Barnard, in Proceedings of IEEE Supercomputing '97 (SC '97), CDROM version (1997).
[10] W. H. Knechtel, G. S. Dusberg, and W. J. Blau, Appl. Phys. Lett. **73**, 1961 (1998).
[11] W. Clauss, D. J. Bergeron, and A. T. Johnson, Phys. Rev. B **58**, 4266 (1998).
[12] J. Bernholc, C. Brabec, M. Buongiorno, A. Maiti, and B. I. Yakobson, Appl. Phys. A **67**, 39 (1998), and references therein.
[13] J. Tersoff, Phys. Rev. Lett. **61**, 2879 (1988).
[14] D. W. Brenner, Phys. Rev. B **42**, 9458 (1990).
[15] A. J. Stone and D. J. Wales, Chem. Phys. Lett. **128**, 501 (1986).
[16] B. I. Yakobson, Appl. Phys. Lett. **72**, 918 (1998).
[17] P. Zhang, P. E. Lammert, and V. H. Crespi, Phys. Rev. Lett. **81**, 5346 (1998).
[18] M. B. Nardelli, B. I. Yakobson, and J. Bernholc, Phys. Rev. Lett. **81**, 4656 (1998).
[19] O. Lourie, D. M. Cox, and H. D. Wagner, Phys. Rev. Lett. **81**, 1638 (1998).
[20] M. Menon, E. Richter, and K. R. Subbaswamy, J. Chem. Phys. **104**, 5875 (1996).
[21] A. M. Rao, E. Richter, S. Bandow, B. Chase, P. C. Eklund, K. A. Williams, S. Fang, K. R. Subbaswamy, M. Menon, A. Thess, R. E. Smalley, G. Dresselhaus, and M. S. Dresselhouse, Science **275**, 187 (1997).
[22] For more details see the review article M. C. Payne *et al.*, Rev. Mod. Phys. **64**, 1045 (1992).
[23] This is similar to the observation reported also by Yakobson *et al.* in Ref. [7].
[24] F. Banhart and P. M. Ajayan, Nature (London) **382**, 433 (1996).